

Article

Optimization of Alachlor Photocatalytic Degradation with Nano-TiO₂ in Water under Solar Illumination: Reaction Pathway and Mineralization

Md. Ashraful Islam Molla ^{1,*}, Mai Furukawa ², Ikki Tateishi ³, Hideyuki Katsumata ² and Satoshi Kaneco ^{2,3}

¹ Department of Applied Chemistry & Chemical Engineering, Faculty of Engineering & Technology, University of Dhaka, Dhaka 1000, Bangladesh

² Department of Chemistry for Materials, Graduate School of Engineering, Mie University, Tsu, Mie 514-8507, Japan; maif@chem.mie-u.ac.jp (M.F.); hidek@chem.mie-u.ac.jp (H.K.); kaneco@chem.mie-u.ac.jp (S.K.)

³ Mie Global Environment Center for Education & Research, Mie University, Tsu, Mie 514-8507, Japan; tateishi@gecer.mie-u.ac.jp

* Correspondence: ashraful.acce@du.ac.bd; Tel.: +88-015-5235-9706

Received: 26 July 2018; Accepted: 17 September 2018; Published: 19 September 2018



Abstract: In the present study, the photocatalytic degradation of alachlor was investigated using TiO₂ under sunlight irradiation. The effects of some operational parameters, such as photocatalyst concentration, temperature, pH, sunlight intensity and irradiation time, were optimized. The kinetics of photodegradation was found to follow a pseudo-first-order kinetic law, and the rate constant at optimal condition is 0.245 min⁻¹. The activation energy (E_a) is 6.4 kJ/mol. The alachlor mineralization can be completed under sunlight irradiation after 10 h. The formations of chloride, nitrate and ammonium ions are observed during the photocatalytic degradation. The eight photoproducts were identified by the GC–MS technique. The photodegradation reaction pathways are proposed based on the evidence of the detected photoproducts and the calculated frontier electron densities of the alachlor structure. The photocatalytic degradation treatment for the alachlor wastewater under solar irradiation is simple, convenient and low cost.

Keywords: photocatalytic degradation; reaction pathways; mineralization; alachlor; sunlight

1. Introduction

Alachlor (IUPAC name: 2-chloro-*N*-(2,6-diethylphenyl)-*N*-(methoxymethyl) acetamide, M.W. = 269.77 g/mol, Figure 1) is a chloroacetanilide herbicide that is applied to the soil to control annual grasses and broadleaf weeds [1]. It is one of the most important agricultural pollutants and is toxic at very low concentrations. Alachlor has been detected in rivers, and drinking and groundwater [2,3]. The allowed maximum concentration level of alachlor for drinking water by the European Union (EU) is set at 0.0001 mg/L [4]. Alachlor causes cancer in laboratory animals [5] and is classified as a group B2 carcinogen by the United States Environmental Protection Agency (EPA) [6]. In addition, alachlor has infertility and genotoxic effects [7,8]. Therefore, the development of efficient and economical techniques to eliminate alachlor is urgently demanded in both scientific and industrial communities.

More recent research efforts have focused on several treatment methods, including ozonation [9], photolysis and photocatalysis [10], photo-Fenton degradation [11], hydrodynamic cavitation [1] and sonochemical reactors [12]. Among these methods, photocatalytic processes offer many advantages for the removal of organic pollutants, such as complete oxidation, no formation of polycyclized products, availability of highly active and affordable catalysts and oxidation of pollutants in the ppb range [13].

However, the photocatalytic oxidation process is typically composed of a UV source and TiO₂ as a photocatalyst. Low-pressure mercury vapor lamps represent an environmental hazard due to the high toxicity of mercury, have relatively short life spans and are energy intensive. These defects make the processing cost-intensive and environmentally problematic. On the other hand, solar photocatalytic water treatment with irradiated semiconductors has been proposed as an effective and environmentally attractive technique for degradation and final mineralization of organic pollutants into CO₂ and inorganic anions [14].

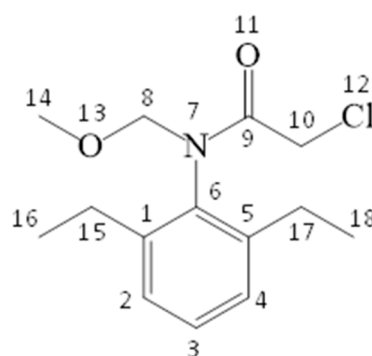


Figure 1. Chemical structure of alachlor.

When nano-TiO₂ is irradiated with UV light (small fraction of solar light, about 4%), valence-band holes (h_{VB}^+) and conduction-band electrons (e_{CB}^-) are produced by Equation (1). The hydroxyl radical ($\bullet OH$), generated through water oxidation by photogenerated valence-band holes, are known to be the most oxidizing species, as shown in Equation (2) [15].



Furthermore, $\bullet OH$ reacts with alachlor, leading to the generation of numerous photoproducts. In the presence of air, other species, such as H₂O₂ or even the superoxide radical ($\bullet O_2^-$), might contribute to the oxidation of the alachlor molecules using Equations (3) and (4).



However, the degradation of alachlor in water by nano-photocatalytic processes under sunlight, which is an effective technique for the removal of recalcitrant contaminants, has been rarely studied. Therefore, in the present work, the photocatalytic degradation of alachlor in water under solar irradiation with nano-TiO₂ was investigated. The effect of factors, including initial concentration of nano-TiO₂, pH of solution, temperature, light intensity and irradiation time, on the degradation of alachlor was investigated. Moreover, the photoproducts from alachlor during this photocatalytic degradation were identified by gas chromatography–mass spectrometry (GC/MS). The degradation pathway is proposed on the basis of the intermediates formed.

2. Experiments

2.1. Materials

The alachlor used in this study was purchased from Wako Pure Chemical Industries Ltd. (HPLC grade >98%; pesticide residue analysis; Osaka, Japan). P-25 TiO₂ powder (80% anatase and 20% rutile, purity 99.9%, particle size 25 nm, surface area 50 m²/g) was purchased from Evonik/Degussa

Chemical Industries Ltd (Essen, Germany). All chemicals were used without further purification. All of the aqueous solutions were prepared with ultrapure water obtained from an ultrapure water system (Advantec MFS Inc., Tokyo, Japan), resulting in a resistivity >18 M Ω cm.

2.2. Photocatalytic Activity and Analyses

A 50 mL aqueous solution containing 10 mg/L alachlor was put into a Pyrex reaction vessel (100 mL capacity). Nano-TiO₂ was added to the solution to produce a concentration of 0.8 g/L. The pH of the solution was 6.0. The temperature was kept constant at 10–60 °C with a water bath. The suspension containing alachlor was irradiated under sunlight illumination. During the irradiation, the nano-TiO₂ was continuously dispersed in the solution by magnetic stirring. In this case, the short ultraviolet radiation ($\lambda < 300$ nm) was filtered out by the vessel wall. The intensity of light was measured by a UV radiometer with a sensor of 320–410 nm wavelength (UVR-400, Iuchi Co., Osaka, Japan). The variation of sunlight intensity for 3 min was less than 5%. After the illumination, the amount of alachlor in the aqueous solution was measured using a high-performance liquid chromatograph equipped with a UV optical detector (GC-7410, GL Science Inc.; Tokyo, Japan) and a separation column ODS-2 (GL Science Inc.; Tokyo, Japan). The elution was monitored at 254 nm. The eluent used was a mixed solvent of acetonitrile and water (65/35, *v/v*). The flow rate of the mobile phase was 1.0 mL/min. The number of experiments for the photocatalytic treatment was greater than three, and the reproducibility of the treatment (relative standard deviation (RSD)) was better relative to RSD 10%.

The progress of mineralization of alachlor was evaluated by measuring the total organic carbon (TOC). The TOC was measured with a Shimadzu TOC analyzer (TOC-VE) based on CO₂ quantification by nondispersive infrared analysis after high-temperature catalytic combustion. Fifty microliters of the sample solution was injected into the TOC analyzer.

The progress of ammonium ion formation was monitored by ionic chromatography using a Shimadzu LC-10AT VP pump equipped with a Shimadzu COD-6A conductivity detector and a Shodex cationic column (IC YK-421). Similarly, the formation of chloride and nitrate ions was also analyzed by ionic chromatography using a Hitachi L-6000 pump equipped with a Hitachi L-3270 conductivity detector and a Hitachi anionic column (#2710-SK-IC; Tokyo, Japan).

The intermediate products were extracted by means of solid-phase extraction. The extraction disk (C18 disk, 3M Empore) was placed in the conventional filtration apparatus and washed with 10 mL of solvent mixture of dichloromethane and ethyl acetate (1:1), 10 mL of methanol and 10 mL of ultrapure water. Then, the sample was percolated through the disk with a flow rate of 5 mL/min under vacuum. The compounds trapped in the disk were collected by using 4 mL \times 5 mL of solvent mixture of dichloromethane and ethyl acetate (1:1) as the eluting system. The fractions were evaporated under a gentle stream of nitrogen to 50 μ L into conical vials, and 1 μ L was injected into a GC–MS instrument in splitless mode. For the analysis of intermediate products, a Shimadzu gas chromatograph and mass spectrometer (GC–MS 5050A) equipped with a DB5 J&W Scientific capillary column (30 m \times 0.25 mm i.d.) was used at the following chromatographic conditions: injector temperature 220 °C, column temperature program 40 °C, 40–200 °C (5 °C/min), 200–210 °C (1 °C/min), 210–280 °C (20 °C/min) and 280 °C (3 min). Helium was used as the carrier gas at 1.5 mL/min. The interface was kept at 280 °C. Qualitative analyses were performed in the electron-impact (EI) mode at 70 eV, using the full scan mode.

Molecular orbital calculations were performed at the single determinant (Hartree–Fock) level for optimization of the minimum energy obtained at the AM1 level. All semi-empirical calculations were performed in MOPAC version 6.01 with a CAChe package (Fujitsu Co. Ltd., Tokyo, Japan). An initial position for a possible •OH radical attack was estimated from calculations of frontier electron densities of the fenitrothion structure. An element of large frontier electron density tends to be attacked by the •OH radical. The mode by which fenitrothion might adsorb onto the TiO₂ surface was estimated from the calculated partial charges of alachlor [16].

3. Results and Discussion

3.1. UV-Vis Spectral Changes

The absorption spectrum changes taking place during the photocatalytic decomposition of alachlor by nano-TiO₂ under sunlight illumination were evaluated. The absorption spectrum decreases after irradiation for 10 min, indicating that alachlor has degraded in the presence of nano-TiO₂ particles with sunlight illumination. Therefore, because it is possible to decompose alachlor by using nano-TiO₂ under sunlight illumination, various factors, including photocatalyst dosage, temperature, pH, light intensity and illumination time, were optimized for the photocatalytic decomposition of alachlor.

3.2. Effect of TiO₂ Dosages on Photodegradation

The effect of the catalyst amount on the photocatalytic degradation was determined in the range of less than 60 mg of the catalyst. The results are shown in Figure 2. The alachlor degradation efficiency increases with an increase in TiO₂ up to 40 mg, and after that value, the increase in catalyst loading scarcely affects the degradation. This observation can be explained in terms of (1) availability of active sites on the catalyst surface and (2) the penetration of light into the suspension. (3) The total active surface area increases with increasing catalyst dosage. At the same time, due to an increase in the turbidity of the suspension, there is a decrease in light penetration as a result of increased scattering effect, and, hence, the photoactivated volume of suspension decreases. (4) Further, at large catalyst loading, it is difficult to maintain the suspension homogeneity due to particle agglomeration, which decreases the number of active sites [17,18]. Since the most effective degradation of alachlor is observed with 40 mg (0.8 g/L) of TiO₂, sequential experiments were performed at this concentration.

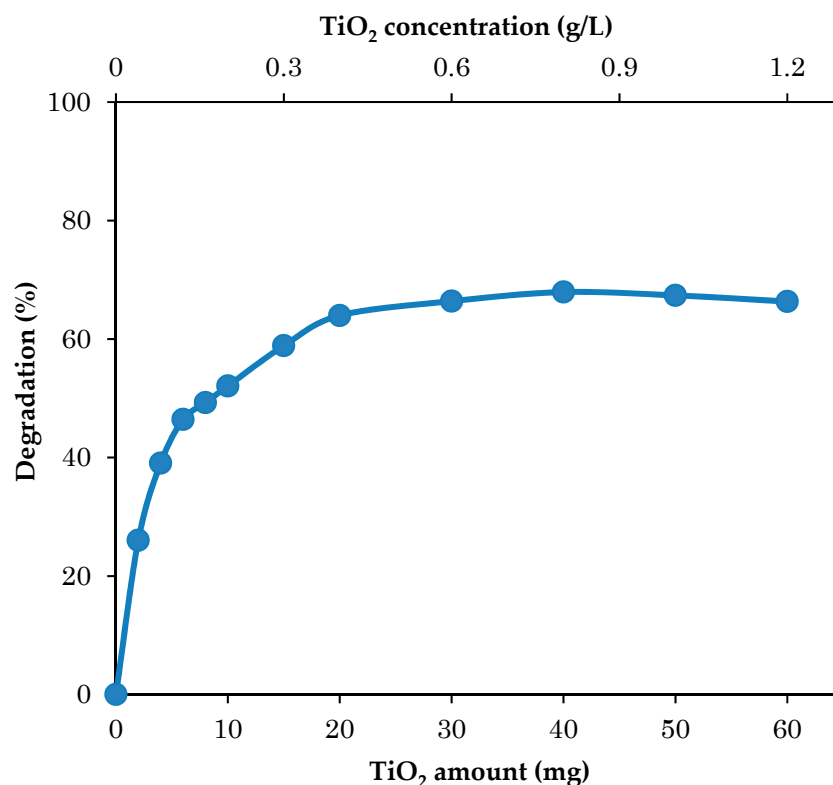


Figure 2. Effect of TiO₂ amount on the solar photocatalytic degradation of alachlor in water. Alachlor: 10 mg/L; irradiation time: 5 min; light intensity: 1.8 mW/cm² (320–410 nm); temperature: 30 °C; pH: 6.

3.3. Effect of Temperature on Photodegradation

The effect of temperature on the solar degradation of alachlor in water using TiO_2 was checked in the range of 10–60 °C. The results are shown in Figure 3. The degradation efficiency of alachlor gradually increases as the temperature increases. Ishiki et al. [19] have investigated the temperature effect for the photodegradation of imazethapyr herbicide in $\text{TiO}_2/\text{H}_2\text{O}$ suspension between 20 and 40 °C, and the herbicide is more easily degraded at lower temperatures in the TiO_2 suspension due to the decrease in the physisorption between the TiO_2 surface and the imazethapyr molecules. By plotting the natural logarithm of the rate constant as a function of reciprocal absolute temperature, a linear behavior is obtained, as drawn in the inset figure in Figure 4.

The activation energy (E_a) of alachlor for photocatalytic degradation is estimated to become 6.4 kJ/mol. It was reported for the TiO_2 photocatalytic degradation of amitrole [20] and probenazole [21] that the activation energy (E_a) is 6.7 and 11.3 kJ/mol, respectively. Since the photoactivation process is irrelevant to thermal activation, the activation energy found is only apparent. Consequently, all subsequent illuminations were performed at 30 °C because of the operating cost for the photodegradation system.

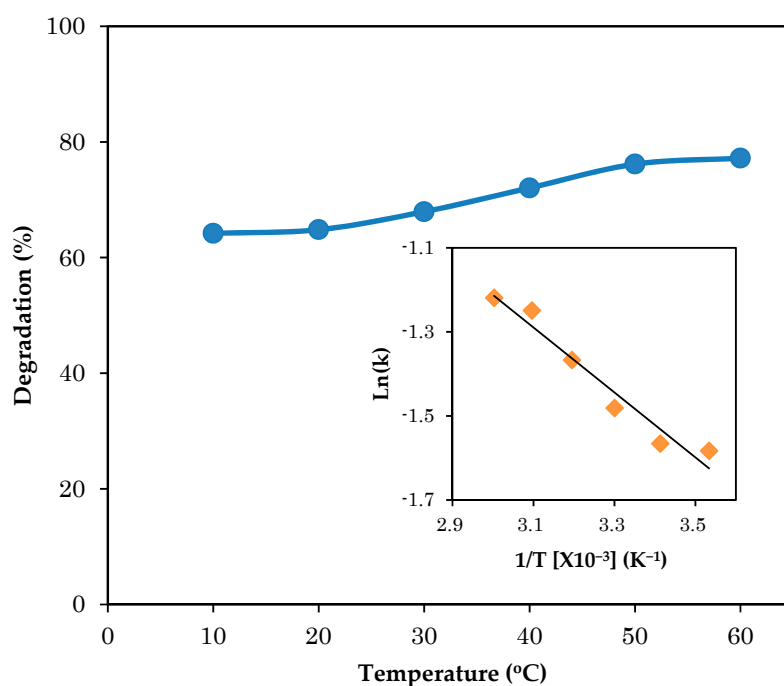


Figure 3. Effect of temperature on the solar photocatalytic degradation of alachlor in water using TiO_2 . Inset figure: plot of $\text{Ln}(k)$ versus $1/T$. Alachlor: 10 mg/L; TiO_2 : 0.8 g/L; light intensity: 1.8 mW/cm² (320–410 nm); irradiation time: 5 min; pH: 6.

3.4. Effect of Initial pH on Photodegradation

The role of initial pH on the degradation efficiency of alachlor was investigated in the pH range of 4–10. As shown in Figure 4, the maximum degradation efficiency is observed at pH 6. The zero-point charge (zpc) pH_{zpc} of TiO_2 particles is around 6 [22]. The TiO_2 catalyst surface will be charged negatively when $\text{pH} > \text{zpc}$, positively when $\text{pH} < \text{zpc}$, and neutrally when $\text{pH} \approx \text{zpc}$. Also, the structural properties of the pollutant will change with pH. The effect of pH on the photocatalytic degradation can be explained as the electrostatic interaction between the catalyst surface and the target material. The adsorption of alachlor onto the TiO_2 surface was estimated from the simulation of molecular partial charges (Table 1). The most negative partial charge atom in the alachlor structure is the nitrogen atom (7N), and the most positive partial charge atom is the

carbon atom (9C). Therefore, the positively charged carbon 9C atom is easily adsorbed in alkaline media ($\text{pH} > 6$) on the TiO_2 surface through electrostatic interaction, and in acidic condition ($\text{pH} < 6$) via the negatively charged nitrogen 7N atom. Therefore, the pH dependence on the degradation efficiency can be attributed to the balance between the induced generation of hydroxyl radicals and the electrostatic repulsion of the alachlor molecule from the photocatalyst surface. The result is consistent with Molla et al. [21]. In the present study, pH 6 was selected for the optimal experimental conditions.

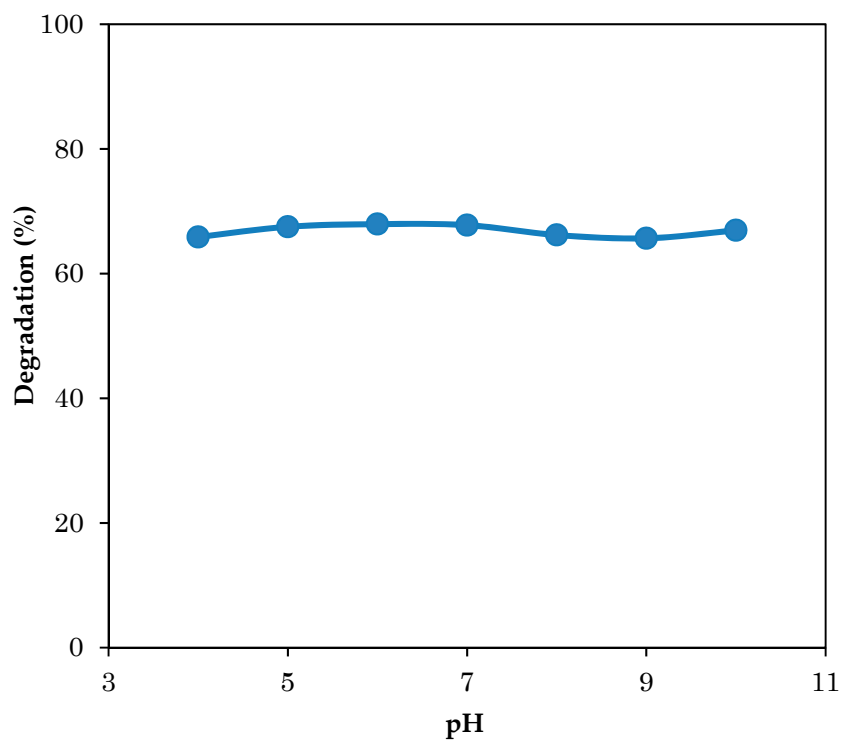


Figure 4. Effect of initial pH on the solar photocatalytic degradation of alachlor in water using TiO_2 . Alachlor: 10 mg/L; TiO_2 : 0.8 g/L; irradiation time: 5 min; light intensity: 1.8 mW/cm^2 (320–410 nm); temperature: 30 °C.

Table 1. Calculations of partial charge (PC) and frontier electron density (FED) foralachlor.

Atom	PC	FED	Atom	PC	FED
C (1)	−0.074	0.174	H (20)	0.133	0
C (2)	−0.138	0.132	H (21)	0.139	0.001
C (3)	−0.141	0.191	H (22)	0.042	0.012
C (4)	−0.140	0.114	H (23)	0.042	0.012
C (5)	−0.055	0.207	H (24)	0.122	0.003
C (6)	0.092	0.331	H (25)	0.122	0.003
N (7)	−0.316	0.233	H (26)	0.062	0
C (8)	0.149	0.116	H (27)	0.062	0
C (9)	0.331	0.125	H (28)	0.114	0.004
C (10)	−0.159	0.088	H (29)	0.102	0.010
O (11)	−0.288	0.065	H (30)	0.102	0.010
Cl (12)	−0.083	0.062	H (31)	0.070	0.001
O (13)	−0.273	0.023	H (32)	0.070	0.001
C (14)	−0.068	0.022	H (33)	0.073	0
C (15)	−0.123	0.009	H (34)	0.105	0.015
C (16)	−0.202	0.001	H (35)	0.105	0.015
C (17)	−0.116	0.018	H (36)	0.067	0.001
C (18)	−0.209	0.001	H (37)	0.067	0.001
H (19)	0.136	0.001	H (38)	0.078	0

3.5. Effect of Light Intensity on Photodegradation

The influence of light intensity on the solar photodegradation ofalachlor in water with TiO₂ was studied (Figure 5). The degradation experiments were performed with various light intensities on sunny and cloudy days. Figure 5 indicates that the increment of light intensity enhances the degradation efficiency. Electron–hole pair (e[−]/h⁺) generation and concentration strongly depend on light intensity [23]. Therefore, the results obtained from the solar photocatalytic degradation ofalachlor in water/TiO₂ suspension are reasonable.

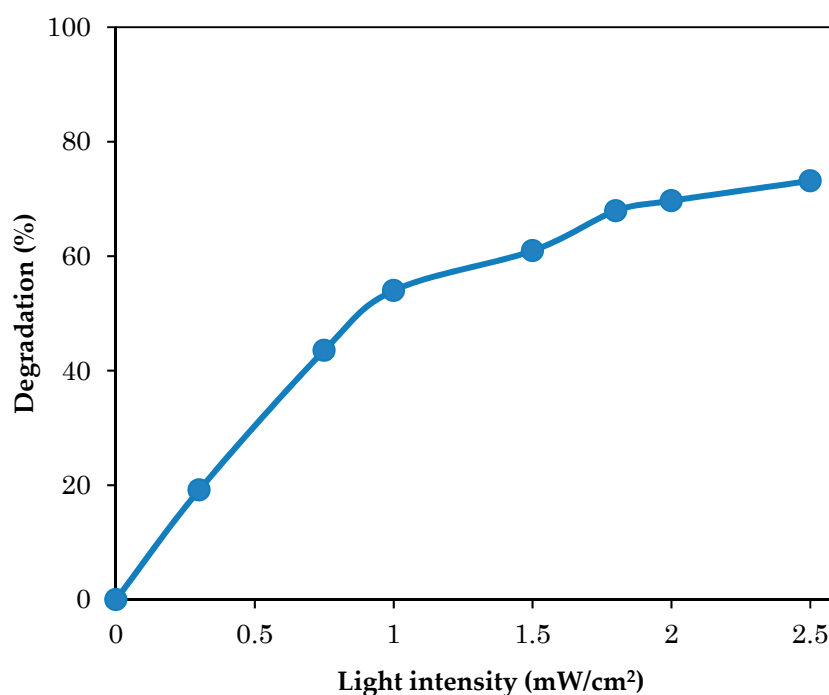


Figure 5. Effect of light intensity on the solar photocatalytic degradation of alachlor in water using TiO₂. Alachlor: 10 mg/L; TiO₂: 0.8 g/L; irradiation time: 5 min; wavelength: 320–410 nm; temperature: 30 °C; pH: 6.

3.6. Effect of Illumination Time

The irradiation time plays an important role in the photocatalytic decomposition of a pollutant. In this work, different irradiation times (2–20 min) for the photocatalytic degradation of alachlor with TiO₂ were investigated. The results are shown in Figure 6. The photocatalytic degradation of alachlor during the first 8 min of irradiation is very fast, and the complete degradation is reached within 20 min. The primary degradation reaction is estimated to follow a pseudo-first-order kinetic law. In order to confirm the speculation, $-\ln(C/C_0)$ was plotted as a function of irradiation time (the inset figure in Figure 6). Since a linear plot is observed in the inset figure, as expected, the degradation of alachlor in the TiO₂ suspension solution follows first-order degradation kinetics. The photodegradation kinetic parameters were determined from the graph, and the pseudo-first-order rate constant k , correlation coefficient R^2 and substrate half-life $t_{1/2}$ are 0.245 min^{-1} , 0.99 and 2.83 min, respectively.

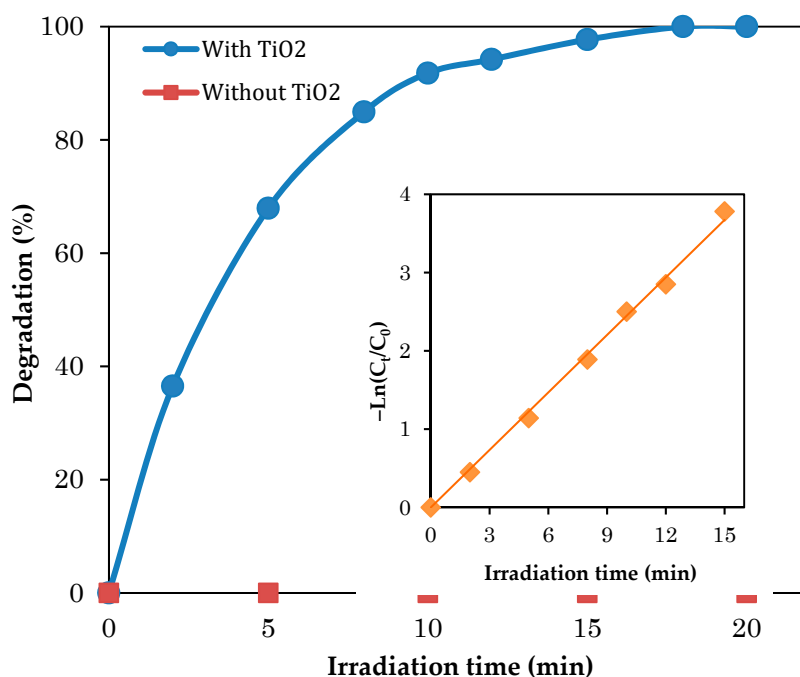
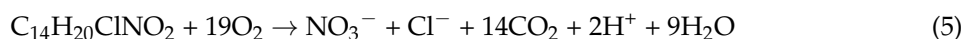


Figure 6. Effect of irradiation time on the solar photocatalytic degradation of alachlor in water using TiO₂. Inset figure: plot of $-\ln(C_t/C_0)$ versus irradiation time. Alachlor: 10 mg/L; TiO₂: 0.8 g/L; light intensity: 1.8 mW/cm² (320–410 nm); temperature: 30 °C; pH: 6.

3.7. Evolution of the Mineralization

The overall stoichiometry for photocatalytic mineralization of alachlor using oxygen as the oxidizing agent in the presence of nano-TiO₂ can be written as follows:



First, the formation of the chloride ion released from alachlor was investigated, as displayed in Figure 7a. The conversion yield to chloride ion increases swiftly with increasing illumination, indicating a very fast degradation/dechlorination stage. Finally, according to mass balance analysis, it is observed that all chlorine atoms are transformed into chloride ions after 60 h of treatment.

The nitrogen released was measured as a combination of ammonium ion and nitrate, but the ammonium ion can be oxidized to nitrate after a long illumination time [24,25]. The formation of ammonium and nitrate ions during the photocatalytic process as a function of reaction time is illustrated in Figure 7b. The amount of ammonium ions increases quickly with the illumination time up to 2 h, and after 2 h the amount increases very slowly. On the contrary, the conversion yield to nitrate ion increases gradually with time until 7 h. The sum of these two products represents the quantitative recovery of organic nitrogen, and about 93% of the initial N is detected as ammonium and nitrate ions after 7 h of illumination time. Therefore, a large fraction of nitrogen atoms from alachlor can be mineralized by this photocatalytic system. This incomplete nitrogen mass balance has frequently been observed in a similar process [26,27]. By comparing the formation efficiencies of chloride, nitrate and ammonium ions, it is seen that the oxidation of the side chain of the alachlor molecule occurs more easily than the cleavage of the ring. From the results, the first step of alachlor photodegradation is mainly the dechlorination.

The progress of the mineralization of the alachlor in water solution was estimated by measuring the total organic carbon (TOC). As shown in Figure 7c, TOC decreases with increasing illumination time up to 10 h, and about 70% reduction of the TOC is achieved.

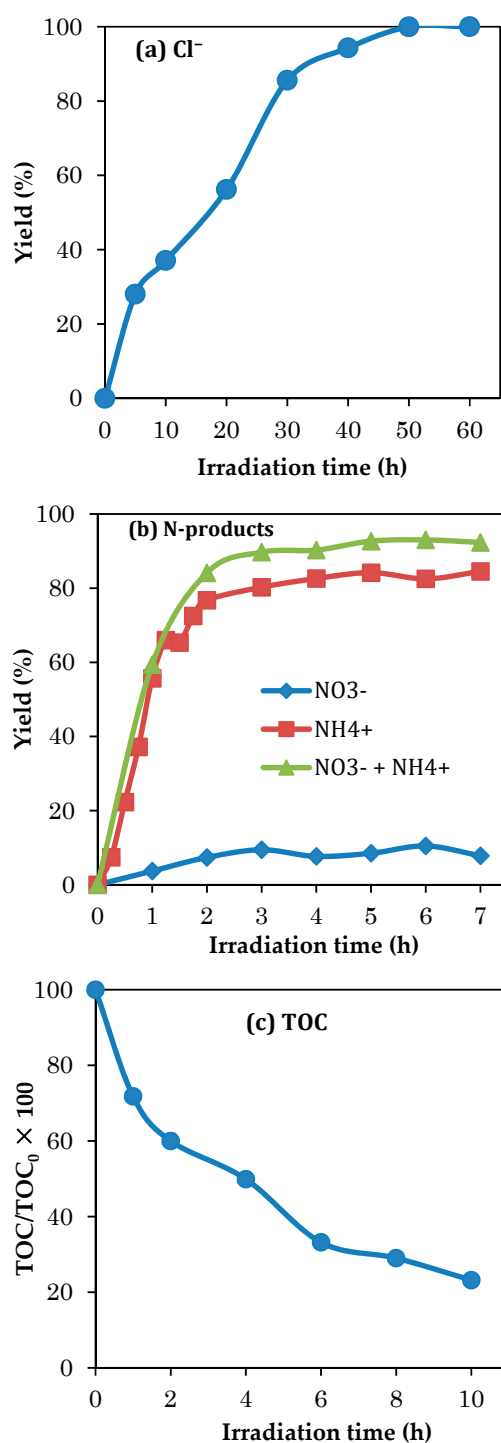


Figure 7. Mineralization during the solar photocatalytic degradation of alachlor. Alachlor: 10 mg/L; irradiation time: 0–60 h; TiO₂: 0.8 g/L; light intensity: 1.8 mW/cm² (320–410 nm); temperature: 30 °C; pH: 6. (a) Cl⁻, (b) N-products and (c) total organic carbon (TOC).

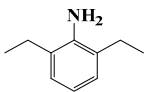
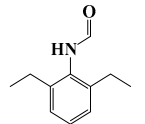
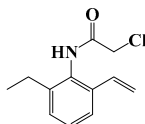
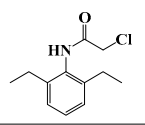
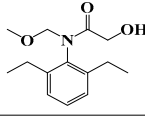
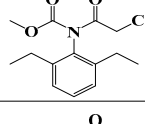
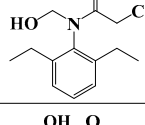
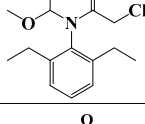
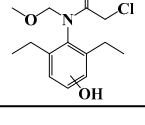
3.8. Photoproducts and Photodegradation Pathway

The intermediate products formed in the photodegradation of alachlor in the aqueous solution after 20 min were evaluated by GC/MS analysis. Eight products were identified by the molecular ion and mass fragment ions. The mass spectral highlights of the photoproducts and their structures are represented in Table 2. Figure 8 illustrates the proposed degradation mechanism of the photocatalytic

process, in which the decay pathways include dechlorination, hydroxylation, dealkylation and scission of the C–O bond and N-dealkylation. The results have been compared to those from previous studies of analogous degradation mechanisms, such as alachlor photocatalysis [11]. From the table, some products (a, b, c, d) are formed due to bond scission or oxidation of the N-methoxymethyl group, and product (e) is characterized by substitution of chlorine with the hydroxyl fraction. The formation of products (f, g, h, i) occur by typical chemical oxidation processes involving alachlor.

From the MOPAC simulation (Table 1), phosphorus (6C) has the largest frontier electron density, with the next one being the nitrogen atom (7N). Hence, these elements would become the most likely sites for attack by $\bullet\text{OH}$.

Table 2. Identified products by GC/MS in the photocatalytic degradation of alachlor.

Product	R _t (min)	Molecular Weight (m/z)	Characteristic Ions (Abundance, %)	Compound
a	13.1	149	57 (100) 134 (54) 149 (39)	
b	15.8	177	57 (100) 162 (86) 177 (79)	
c	17.2	223	146 (100) 174 (56) 223 (40)	
d	18.3	225	147 (18) 176 (100) 225 (10)	
e	21.7	251	160 (100) 174 (62) 202 (48)	
f	23.0	283	174 (100) 206 (32) 248 (37)	
g	23.6	255	146 (100) 174 (74) 223 (27)	
h	25.7	285	176 (100) 204 (61) 253 (36)	
i	27.1	285	176 (100) 204 (61) 253 (32)	

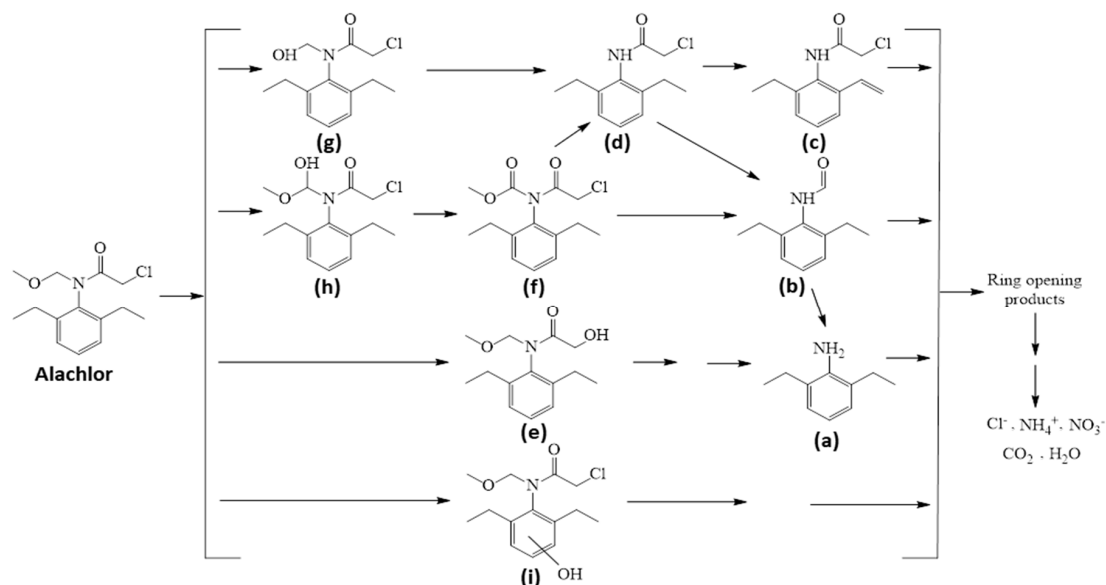


Figure 8. Proposed solar photodegradation pathway of alachlor with TiO_2 .

4. Conclusions

The solar photocatalytic purification of water containing alachlor was performed in titanium dioxide. The photodegradation follows first-order kinetics, and complete disappearance is observed after 20 min under optimum conditions. The half-life ($t_{1/2}$) and the activation energy (E_a) are 2.83 min and 6.4 kJ/mol, respectively. Almost 100% of the organic carbon is converted into CO_2 after 10 h of illumination. The heteroatoms Cl and N are released as chloride ions and ammonium and nitrate ions, respectively. Eight kinds of photoproducts of alachlor during the photocatalytic system were identified. The degradation pathway of alachlor is proposed based on the detected byproducts under the optimum conditions.

Author Contributions: M.A.I.M. and S.K. conceived and designed the experiments. M.A.I.M. performed the experiments and wrote the paper. M.F., I.T. and H.K. analyzed the results and advised the project.

Funding: The present research was partly supported by Grant-in-Aid for Scientific Research (C) 18K11709 from the Ministry of Education, Culture, Sports, Science, and Technology of Japan.

Acknowledgments: All experiments were conducted at Mie University. Any opinions, findings, conclusions or recommendations expressed in this paper are those of the authors and do not necessarily reflect the view of the supporting organizations.

Conflicts of Interest: The authors declare no conflict of interest.

References

1. Wang, X.; Zhang, Y. Degradation of alachlor in aqueous solution by using hydrodynamic cavitation. *J. Hazard. Mater.* **2009**, *161*, 202–207. [[CrossRef](#)] [[PubMed](#)]
2. Ramesh, A.; Maheswari, S.T. Dissipation of alachlor in cotton plant, soil and water and its bioaccumulation in fish. *Chemosphere* **2004**, *54*, 647–652. [[CrossRef](#)] [[PubMed](#)]
3. Rivera, K.K.P.; de Luna, M.D.G.; Suwannaruang, T.; Wantala, K. Photocatalytic degradation of reactive red 3 and alachlor over uncalcined Fe-TiO₂ synthesized via hydrothermal method. *Desalin. Water Treat.* **2016**, *57*, 22017–22028. [[CrossRef](#)]
4. Gabaldón, J.A.; Cascales, J.M.; Maqueira, A.; Puchades, R. Rapid trace analysis of alachlor in water and vegetable samples. *J. Chromatogr. A* **2002**, *963*, 125–136. [[CrossRef](#)]
5. Horberg, G. Risk, science and politics, Alachlor regulation in Canada and the United States. *Can. J. Political Sci.* **1990**, *23*, 257–277. [[CrossRef](#)]

6. *Special Review of Certain Pesticide Products—Alachlor*; Document No. PB85-175503; Office of Pesticide Programs, Environmental Protection Agency: Springfield, VA, USA, 1985.
7. Osano, O.; Admiraala, W.; Klamerc, H.J.C.; Pastorc, D.; Bleekera, E.A.J. Comparative toxic and genotoxic effects of chloroacetanilides, formamidines and their degradation products on *Vibrio fischeri* and *Chironomus riparius*. *Environ. Pollut.* **2002**, *119*, 195–202. [[CrossRef](#)]
8. Grizard, G.; Ouchchane, L.; Roddier, H.; Artonne, C.; Sion, B.; Vasson, M.-P.; Janny, L. In vitro alachlor effects on reactive oxygen species generation, motility patterns and apoptosis markers in human spermatozoa. *Reprod. Toxicol.* **2007**, *23*, 55–62. [[CrossRef](#)] [[PubMed](#)]
9. Li, H.Y.; Qu, J.H.; Liu, H.J. Decomposition of alachlor by ozonation and its mechanism. *J. Environ. Sci.* **2007**, *19*, 769–775. [[CrossRef](#)]
10. Bahena, C.L.; Martinez, S.S. Photodegradation of chlorbromuron, atrazine, and alachlor in aqueous systems under solar irradiation. *Int. J. Photoenergy* **2006**, *2006*, 81808. [[CrossRef](#)]
11. Katsumata, H.; Kaneco, S.; Suzuki, T.; Ohta, K.; Yobiko, Y. Photo-Fenton degradation of alachlor in the presence of citrate solution. *J. Photochem. Photobiol. A Chem.* **2006**, *180*, 38–45. [[CrossRef](#)]
12. Wayment, D.G.; Casadonte, D.J., Jr. Frequency effect on the sonochemical remediation of Alachlor. *Ultrason. Sonochem.* **2002**, *9*, 251–257. [[CrossRef](#)]
13. DeviPriya, S.; Yesodharan, S. Photocatalytic degradation of pesticide contaminants in water. *Sol. Energy Mater. Sol. Cells* **2005**, *86*, 309–348. [[CrossRef](#)]
14. Fujishima, A.; Rao, T.; Tryk, D. Titanium dioxide photocatalysis. *J. Photochem. Photobiol. A Chem.* **2000**, *1*, 1–21. [[CrossRef](#)]
15. Kansal, S.K.; Ali, A.H.; Kapoor, S. Photocatalytic decolorization of biebrich scarlet dye in aqueous phase using different nanophotocatalysts. *Desalination* **2010**, *259*, 147–155. [[CrossRef](#)]
16. Kenichi, F.; Teijiro, Y.; Chikayoshi, N.; Haruo, S. Molecular-orbital theory of orientation in aromatic, heteroaromatic, and other conjugated molecules. *J. Chem. Phys.* **1954**, *22*, 1433–1442.
17. Behnajady, M.A.; Modirshahla, N.; Hamzavi, R. Kinetic study on photocatalytic degradation of C.I. Acid Yellow 23 by ZnO photocatalyst. *J. Hazard. Mater. B* **2006**, *133*, 226–232. [[CrossRef](#)] [[PubMed](#)]
18. Daneshvar, N.; Salari, D.; Khataee, A.R. Photocatalytic degradation of azo dye acid red 14 in water on ZnO as an alternative catalyst to TiO₂. *J. Photochem. Photobiol. A Chem.* **2004**, *162*, 317–322. [[CrossRef](#)]
19. Ishiki, R.R.; Ishiki, H.M.; Takashima, K. Photocatalytic degradation of imazethapyr herbicide at TiO₂/H₂O interface. *Chemosphere* **2005**, *58*, 1461–1469. [[CrossRef](#)] [[PubMed](#)]
20. Molla, M.A.I.; Ahsan, S.; Tateishi, I.; Furukawa, M.; Katsumata, H.; Suzuki, T.; Kaneco, S. Degradation, kinetics, and mineralization in solar photocatalytic treatment of aqueous amitrole solution with titanium dioxide. *Environ. Eng. Sci.* **2018**, *35*, 401–407. [[CrossRef](#)]
21. Molla, M.A.I.; Furukawa, M.; Tateishi, I.; Katsumata, H.; Kaneco, S. Solar photocatalytic decomposition of Probenazole in water with TiO₂ in the presence of H₂O₂. *Energy Sources A Recov. Util. Environ. Eff.* **2018**, *40*, 2432–2441. [[CrossRef](#)]
22. Yang, H.G.; Li, C.Z.; Gu, H.C.; Fang, T.N. Rheological behavior of titanium dioxide suspensions. *J. Colloid Interface Sci.* **2001**, *236*, 96–103. [[CrossRef](#)] [[PubMed](#)]
23. Mirmasoomi, S.R.; Ghazi, M.M.; Galedari, M. Photocatalytic degradation of diazinon under visible light using TiO₂/Fe₂O₃ nanocomposite synthesized by ultrasonic-assisted impregnation method. *Sep. Purif. Technol.* **2017**, *175*, 418–427. [[CrossRef](#)]
24. Bosen, E.M.; Schroeter, S.; Jacobs, H.; Broekaet, J.A.C. Photocatalytic degradation of ammonia with TiO₂ as photocatalyst in the laboratory and under the use of solar radiation. *Chemosphere* **1997**, *35*, 1431–1445. [[CrossRef](#)]
25. Pramauro, E.; Vincenti, M.; Augugliaro, V.; Palmisano, L. Photocatalytic degradation of monuron in aqueous titanium dioxide dispersions. *Environ. Sci. Technol.* **1993**, *27*, 1790–1795. [[CrossRef](#)]
26. Sakkas, V.A.; Dimou, A.; Pitarakis, K.; Mantis, G.; Albanis, T. TiO₂ photocatalyzed degradation of diazinon in an aqueous medium. *Environ. Chem. Lett.* **2005**, *3*, 57–61. [[CrossRef](#)]
27. Mahmoodi, N.M.; Arami, M.; Limaee, N.Y.; Gharanjig, K. Photocatalytic degradation of agricultural N-heterocyclic organic pollutants using immobilized nanoparticles of titania. *J. Hazard. Mater.* **2007**, *145*, 65–71. [[CrossRef](#)] [[PubMed](#)]

